

Multiband magnetism and superconductivity in Fe-based compounds

V. CVETKOVIC^(a) and Z. TESANOVIC

Department of Physics and Astronomy, The Johns Hopkins University - Baltimore, MD 21218, USA

received 12 November 2008; accepted in final form 18 January 2009

published online 13 February 2009

PACS 74.20.-z – Theories and models of superconducting state

PACS 75.30.Fv – Spin-density waves

PACS 71.45.Lr – Charge-density-wave systems

Abstract – Recent discovery of superconductivity in Fe-based layered compounds may have opened a new pathway to the room temperature superconductivity. A model Hamiltonian describing FeAs layers is introduced, highlighting the crucial role of puckering of As atoms in promoting *d* electron itinerancy and warding off large local-moment magnetism of Fe ions, the main enemy of superconductivity. Quantum many-particle effects in charge, spin and multiband channels are explored and a nesting-induced spin density-wave order is found in the parent compound. We argue that this largely itinerant antiferromagnetism and high T_c itself are essentially tied to the multiband nature of the Fermi surface.

Copyright © EPLA, 2009

Recently, a surprising new path to room-temperature superconductivity might have been discovered. The quaternary compound LaOFeP was already known to become superconductor below 7 K [1], when its doped sibling LaO_{1-x}F_xFeAs turned out to have unexpectedly high $T_c = 26$ K [2]. Even higher T_c 's were found by rare-earths (RE) substitution, reaching the current record of 55 K [3]. These are the first non-cuprate superconductors exhibiting such high T_c 's.

The surprise here is that the most prominent characteristic of iron is its magnetism. By conventional wisdom, the superconductivity in RE-OFeAs compounds is unexpected, all the more so since it apparently resides in FeAs layers. Following standard ionic accounting, rare-earths are 3⁺, while As and O are 3⁻ and 2⁻, respectively. One then expects Fe to be in its 2⁺ configuration, two of its 4s electrons given away to fill As and O *p*-orbitals, with assistance from a single rare-earth atom. The remaining six *d* electrons fill atomic orbitals of Fe in the overall tetragonal As/O environment (fig. 1); the lower three *t*_{2g} orbitals should be filled while the upper two *e*_g orbitals should be empty. However, the Coulomb interactions intervene via Hund's rule. The simplest realization of this is to fully occupy a low *t*_{2g} orbital while storing the remaining four electrons into the spin-up states. The result is a total spin $S = 2$ of Fe²⁺, with the associated local magnetic moment and likely magnetism in the parent compounds. This is the

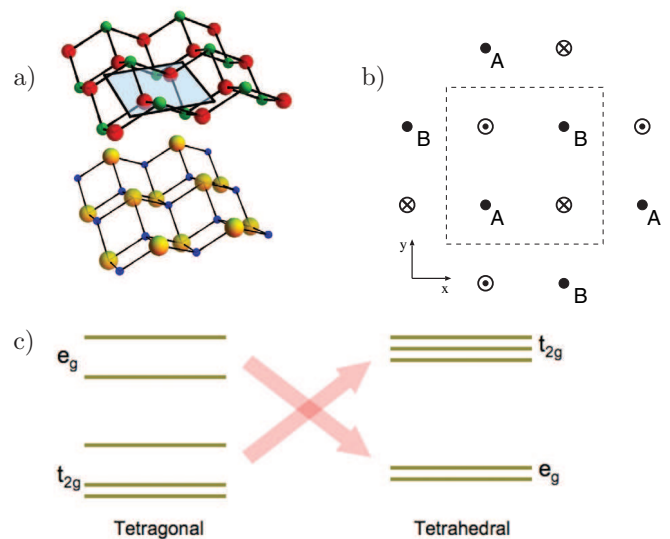


Fig. 1: (Colour on-line) (a) The structure of the parent compound, with FeAs layer (Fe: red, As: green) on top of REO layers (RE: yellow, O: blue); the blue square in the FeAs plane corresponds to the “planar” unit cell (b). We denote two Fe atoms with A and B, while the two As atoms that are displaced up and down with respect to the layer are represented by dotted and crossed circles respectively. (c) The evolution of *d*-orbital energy levels from the tetragonal to tetrahedral crystal field environment. The puckering of FeAs planes results in the situation which is “in between”, placing all *d*-orbitals near the Fermi level.

^(a)E-mail: vladimir@pha.jhu.edu

situation similar to manganese, the Fe's nearest relative, whose five d electrons feel the full brunt of Hund's rule and typically line up into a large spin state, and very different from copper, where d -orbitals are either fully occupied or contain only a single d -hole, as in the parent state of cuprate superconductors. All told, the circumstances are hardly hospitable to any superconductivity, let alone a high-temperature one.

In this paper, we first argue that the above Hund's rule route to large local moment magnetism is derailed by significant banding effects, promoting enhanced itinerancy for most Fe d electrons. We show how such itinerancy arises from the combination of two factors: a sizeable overlap among Fe and As atomic orbitals and the distortion of the overall tetragonal structure into a locally near-tetrahedral environment for Fe ions, *both* generated by the *crucial* "puckering" of As atoms out of the FeAs planes (fig. 1). The puckering rearranges the crystal field levels so that $E_{t_{2g}} \sim E_{e_g}$ —the situation "in between" the purely tetragonal ($E_{t_{2g}} < E_{e_g}$) and the purely tetrahedral ($E_{t_{2g}} > E_{e_g}$)—thus bringing *all* d -orbitals into a close proximity of the Fermi level E_F , and maximizes direct overlap between Fe d - and As p -orbitals. The end result are numerous bands crossing E_F and a multiply connected Fermi surface, containing both electron and hole sections. We introduce a two-dimensional tight-binding model which captures the relevant features of this multiband problem. Next, we argue that large number of broad bands and the absence of large local Fe moments betrays not only the failure of the atomic Hund's rule but, via the enhanced metallic screening, the *absence of strong local correlations in general*. This implies the key role for the nesting properties and we present an *analytic* calculation of various responses relevant to this multiband problem. These responses allow us to account for the observed weak anti-ferromagnetic ordering in parent materials and provide strong clues about the superconducting mechanism itself. In this sense, the Fe-based high- T_c superconductors differ from the *hole*-doped cuprates and are likely more closely related to either the *electron*-doped cuprates or other weakly to moderately correlated superconductors.

The parent compound of the Fe-based superconductors has a ZrCuSiAs-type structure [4] (fig. 1). The Fe atoms lie in a plane, same as O atoms precisely above them, in the adjacent REO layer. In contrast, the RE and As atoms (also located above each other) are puckered out of plane in a checkerboard fashion. The amount of puckering is significant, turning the in-plane tetragonal structure into the nearly-tetrahedral one (the angle of the FeAs bond with respect to the vertical is 58.8° as compared to 54.7° for a tetrahedron [5]). This has important consequences for promoting banding and rich orbital content near E_F .

The available electronic structure calculations of LaOFeP [6], and of LaOFeAs, doped and undoped [7,8], consistently convey the key information that all five Fe $3d$ bands of are located at the Fermi level, in stark contrast with the cuprates. These bands hybridize with $4p$ orbitals

of As/P located far below the Fermi level. There are five sections of the Fermi surface: two hole concentric, near-cylindrical ones around the Γ -point, two electron elliptical ones, centered around the M -point, and a hole band with a spherical Fermi surface around the Z -point. Given the fact that the last one vanishes upon doping [8], and that the relevant physics appear to be two-dimensional, we will ignore this Fermi surface and neglect the interlayer couplings altogether. This idea is used in other works which aim to recreate the band structure [9–12].

To illustrate the key role of the puckering of As atoms on the electronic structure, let us first consider the hypothetical situation with no puckering. The tetragonal crystal field splitting pushes t_{2g} orbitals below the e_g orbitals. In this arrangement, the overlap of t_{2g} orbitals with the neighbouring As p -orbitals either vanishes by symmetry or is very small, the *only* source of broadening for these bands being the direct overlap of two d -orbitals on neighbouring Fe. The e_g bands, on the other hand, directly couple to the $4p$ -orbitals of As, but, since the p -orbitals are deep below the Fermi level, this coupling only pushes the e bands further up, increasing the crystal field gap. The consequence is that such a material should likely be a band insulator, turning into a local moment magnet once the Coulomb effects and Hund's rule are turned on. A sizeable puckering changes the situation dramatically: first, the Fe crystal field environment turns to near-tetrahedral instead of the tetragonal. In the nearly-tetrahedral case of real FeAs layers, the t_{2g} orbitals are slightly above e_{2g} , and the overlap due to the band formation makes *all* five bands important. The banding is the other crucial consequence of the puckering: since the $p_{x,y}$ -orbitals are not entirely in the Fe plane, the overlap between these and $d_{xz,yz}$ -orbitals becomes significant, providing the dominant contribution to electron/hole hopping.

Based on the above arguments, we construct a tight-binding model incorporating the hoppings to the nearest neighbours. This model reflects the key qualitative features of the electronic structure calculations [7,8], and it can serve as the realistic platform for further *analytic* calculations. Even such a simplified model must include *all* five d bands and is defined by

$$H = H_0 + H_t + H_{int}, \quad (1)$$

$$H_0 = \sum_{i,\alpha} \epsilon^{(\alpha)} d_i^{(\alpha)\dagger} d_i^{(\alpha)} + \sum_{j,\beta} \epsilon^{(\beta)} p_j^{(\beta)\dagger} p_j^{(\beta)}, \quad (2)$$

$$H_t = \sum_{i,j,\alpha,\beta} t_{(\alpha,\beta)} d_i^{(\alpha)\dagger} p_j^{(\beta)} + \sum_{i,i',\alpha,\alpha'} t_{(\alpha,\alpha')}^{Fe} d_i^{(\alpha)\dagger} d_{i'}^{(\alpha')} + \sum_{j,j',\beta,\beta'} t_{(\beta,\beta')}^{As} p_j^{(\beta)\dagger} p_{j'}^{(\beta')} + \text{h.c.}, \quad (3)$$

where H_0 describes local $3d$ - and $4p$ -orbitals, and H_t accounts for various hoppings. H_{int} is the interaction term which is discussed shortly. The operator $d_i^{(\alpha)}$ annihilates an electron in orbital α on Fe site i , and analogously,

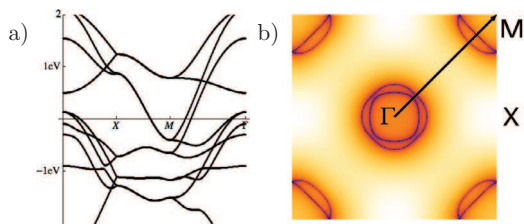


Fig. 2: (Colour on-line) The band structure (a), and the Fermi surfaces (b) following from the tight-binding Hamiltonian (1), and using the parameters of the tight-binding fit.

$p_j^{(\beta)}$ annihilates an electron on site j in orbital β . The summation over α takes into account all five Fe $3d$ -orbitals, and the summation over β involves all three bands $p_{x,y,z}$.

We find the orbital energies and hoppings (all in eV's):

α	$x^2 - y^2$	z^2	xy	xz	β	x	z
ϵ_α	-0.85	-1.4	-1.1	-1.15	ϵ_β	-4.0	-4.0
$t_{\alpha,\alpha}^{Fe}$	-0.55	-0.5	-1.6	-0.55	$t_{\beta,\beta}^{As}$	-0.8	-0.45
$t_{\alpha,x/y}$	0.65	-1.4	1.5	3.2			
$t_{\alpha,z}$	2.1	1.25		0.7			

The interband couplings are not tabulated and their values are $t_{z^2,xy}^{Fe} = 0.1$, $t_{xz,yz}^{Fe} = -0.75$, and $t_{x,y}^{As} = 0.8$.

The levels ϵ_α reflect our previous discussion of the crystal field splitting: $E_{t_{2g}} \sim E_{e_g}$ on the scale of t 's. The hoppings reveal that the puckering of As atoms promoted $d_{xz/yz}$ bands to the physically most relevant ones, their coupling to the $4p$ -orbitals being the strongest. These bands provide dominant content of the electronic states at E_F , where they get mixed with the other states. In addition, significant mixing of different d -orbitals with opposite parity relative to the FeAs planes further reinforces the need to include the full d -orbital manifold into the basic description.

Figure 2 shows the band structure and the Fermi surface(s) following from (1). The key features of the Fermi surface are faithfully reproduced, with the central hole pockets nearly circular. Around the M -point, the two electron pockets have elliptical shape and do not interact at the crossing points located at the edges of the Brillouin zone.

This brings us to H_{int} in (1). The above picture of puckered As atoms, promoting the bunching of local d levels of Fe and their large overlap with As p -orbitals, indicates that the d bands are near their optimum width, given the restrictions of dealing with $3d$ electrons and $4p$ levels far below of E_F . This reduces the importance of Hund's rule and points to the d electron itinerancy, rather than local atomic (ionic) correlations, as the most relevant feature. Indeed, this is consistent with the neutron scattering experiments [13], observing weak antiferromagnetism in the parent compound below 150 K instead of the large local moment magnetism expected in Hund's rule limit. The AF order is suppressed by doping and ultimately vanishes in the superconducting state. This suggests that

H_{int} should generically be comparable or smaller in size than H_t (1). For example, in the simple single-band Hubbard model, with nearly circular (or spherical) Fermi surface, too large on-site repulsion U leads to the ferromagnetic Stoner instability, an itinerant prelude to the local moment formation dictated by Hund's rule. We thus expect that the main effects of H_{int} can be understood by a detailed analysis of enhanced spin, charge and interband responses of the non-interacting part of H (1).

With this in mind, we note that pockets of the Fermi surface (fig. 2) can be viewed as radial/elliptical distortions of a circle, two of such ideal (hole) pockets located at Γ and two (electron) at M points. If these distortions are not too extreme, various responses can be evaluated *analytically*. Where comparison is possible, our analytic results agree with the numerical ones in refs. [8,11,12].

We first look at the spin-susceptibility, and analyze how near-nesting can lead to SDW order. We make assumptions about the Fermi surfaces and separate the most important contributions. While some nesting takes place *within* slightly deformed circular Fermi surfaces, the main contribution to the enhanced response arises from similarly shaped *hole and electron* pockets, followed by a less important one arising from different hole-hole and electron-electron pockets. This is easily appreciated by nothing that, for our *idealized* circles, the electron-hole nesting leads to a *divergent* contribution to the electron-hole propagator. So, we concentrate on the spin-susceptibility $\chi_s(\mathbf{q}, \omega)$ where one the particle propagators corresponds to the hole band at the Γ -point with a circular Fermi surface and Fermi momentum k_F , and the electron band forming a slightly elliptically deformed Fermi surface centered around M -vector (fig. 2). The dispersions are

$$\epsilon_{\mathbf{k}}^{(e)} = \frac{1}{2m_e} \left[\frac{k_x^2}{(1+\xi)^2} + \frac{k_y^2}{(1+\eta)^2} - k_F^2 \right], \quad (4)$$

$$\epsilon_{\mathbf{l}}^{(h)} = \frac{k_F^2 - l^2}{2m_h}, \quad (5)$$

with $m_{e,h}$ being the mass of the electron/hole band. For simplicity we assume $m_e = m_h$. Wave vector \mathbf{k} is given relative to the M point in the case of the electron band, while \mathbf{l} is defined with respect to Γ . Parameters ξ and η are tied to the eccentricity and the size of electron Fermi ellipse. Below, we evaluate the particle-hole (p-h) bubble due to the near-nesting of only one hole and one electron band. Our results are universal, generally applicable to any situation involving elliptical Fermi surfaces, and particularly relevant for FeAs, where one has to sum contributions due to nesting of each individual hole and electron band.

If the two bands were identical ($\xi = \eta = 0$), the real part of the susceptibility would simply be given by $\chi'_0(\mathbf{q}, \omega = 0) = (m_e/\pi) \log(\Lambda/|\mathbf{q} - \mathbf{M}|)$, where Λ is the UV band cut-off. A logarithmic singularity occurs when $\mathbf{q} = \mathbf{M}$ due to the perfect nesting. The nesting in FeAs is not perfect due to small distortions, and this singularity is cut off.

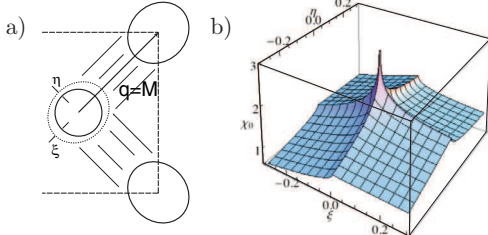


Fig. 3: (Colour on-line) The arrangement of Fermi surfaces with elliptical bands at the corners of the Brillouin Zone show in fig. 2(a), and the regularization of the singular part of the susceptibility due to the elliptical distortion of the electronic Fermi surface (b).

Still, it appears nevertheless that this particular response at $\mathbf{q}=\mathbf{M}$ is the strongest incipient instability of our system. If H_{int} is overall repulsive and not extremely weak, say modelled as a Hubbard repulsion on Fe sites, this instability will produce the SDW ground state at the *commensurate* wave vector $\mathbf{q}=\mathbf{M}$. It seems natural to associate this Fermi surface instability with the observed weak AFM order of the parent compound [13].

To appreciate how the deformation of the electron Fermi surface cuts off the singularity, we now find the explicit expression for this more general situation. There are two different cases, depending on whether the two Fermi surfaces intersect after one has been moved by \mathbf{M} . If they do not intersect (equivalent to $\xi\eta > 0$), the susceptibility is

$$\chi'_0(\mathbf{q}=\mathbf{M}, \omega=0) = 4 \frac{m_e}{2\pi} \frac{(1+\xi)(1+\eta)}{\sqrt{\Xi\Upsilon}} \times \left\{ \log \left[\frac{\Lambda}{k_F} \sqrt{2\Xi\Upsilon} \sqrt{\Xi+\Upsilon+2\sqrt{\Xi\Upsilon}} \right] - \log(\Xi\Upsilon) - \log \left[|\Xi\Upsilon - \Xi - \Upsilon| + \sqrt{\Xi\Upsilon(\Xi-2)(\Upsilon-2)} \right] \right\}, \quad (6)$$

where $\Xi = 1 + (1+\xi)^2$ and $\Upsilon = 1 + (1+\eta)^2$.

Clearly, it is the last two term which cause the nesting divergence in the limit when the ellipse transforms to a circle ($\xi \rightarrow 0, \eta \rightarrow 0$). When the Fermi surfaces intersect ($\xi\eta < 0$), the last two logarithms in (6) should be replaced by $-\log(2+\xi+\eta) - \log|\Xi - \Upsilon|$. This term is responsible for the singularity in this case. The divergent behavior of the real part of the susceptibility is shown in fig. 3.

Our analysis of the divergent part of the susceptibility was centered on the case when $\mathbf{q}=\mathbf{M}$, and the question remains whether that is the global maximum. It is trivial to demonstrate that the first derivative at $\mathbf{q}=\mathbf{M}$ vanishes in all directions. Therefore, one has to look for the sign of the second derivative in order to determine the nature of the extremum at $\mathbf{q}=\mathbf{M}$. While the general treatment of the problem will be presented elsewhere [14], we illustrate the situation by two circular Fermi surfaces with slightly different radii, k_F , and $k_F(1+\xi)$. The susceptibility due to the nesting of these Fermi surfaces is compared for the cases when $\mathbf{q}=\mathbf{M}$, and $\mathbf{q}=\mathbf{M}+k_F\xi\mathbf{n}$, with \mathbf{n} being an arbitrary unit vector. The former corresponds to concentric Fermi surfaces, the latter to two surfaces touching

each other. The susceptibility in the former case is

$$\chi'_0(\mathbf{q}=\mathbf{M}, 0) = \frac{4m_e}{2\pi} \frac{(1+\xi)^2}{\Xi} \log \left[\frac{\Lambda}{k_F|\xi|} \sqrt{\frac{2\Xi}{(2+\xi)^2}} \right] \quad (7)$$

and the result for touching circles is obtained by replacing the argument under the square root by 2. This is always slightly larger than the susceptibility following from eq. (7), regardless the value of ξ . Such a result implies a different ordering vector $\tilde{\mathbf{q}}=\mathbf{M}+k_F\xi\mathbf{n}$, albeit only in a continuum theory. Our system is on a lattice, and \mathbf{M} is commensurate with the reciprocal lattice, hence any instability at that wave vector will be enhanced by Umklapp processes, whereas this is not true for other incommensurate wave vectors such as $\tilde{\mathbf{q}}$. Furthermore, we may argue that two Fermi surfaces touching should not produce any unexpected divergences in the p-h channel, by observing the analytic expression (6) when ξ or $\eta=0$.

Equation (6) can be applied to all the pairs of hole/electron bands in the band structure. For the UV cut-off we choose the inverse lattice spacing. We now compare the relative values for the doped and parent systems, with the help from the band structure calculations. For the undoped parent system, we estimate [6] $\xi_1 \approx 0.27$, $\eta_1 \approx 0.45$, $\xi_2 \approx 0.00$, and $\eta_2 \approx 0.14$, which yields $\chi'_0 \approx 5.3m_e$ at $\mathbf{q}=\mathbf{M}$. Doping moves E_F upwards, *increasing* the electron, and *shrinking* the hole Fermi surfaces. The corresponding surfaces are now further apart, so the susceptibility is smaller. We estimate [8] $\xi_1 \approx 0.72$, $\eta_1 \approx 1.11$, $\xi_2 \approx 0.35$, and $\eta_2 \approx 0.65$, giving $\chi'_0 \approx 3.8m_e$ at $x=0.1$. Similar estimate is obtained by using our tight-binding band structure of fig. 2. This is quite a bit smaller than the undoped value, and suggests rapid suppression of our SDW upon doping, as observed experimentally [13].

The SDW/AF order at $\mathbf{q}=\mathbf{M}$ discussed above and observed in experiments, could in principle also be interpreted in the *local* spin picture, as arising from the direct and indirect superexchange between Fe atoms. The direct superexchange J_1 is generated by the overlap of 3d orbitals of neighbouring atoms, *i.e.*, overlap between A and B atoms. Two A(B) atoms, in contrast, have an insignificant direct overlap. However, from our band structure we know that bands $d_{xz,yz}$ hybridize with $4p$ -orbitals of As. Let us for example take one A atom in a unit cell in fig. 1, and consider its overlap with its next neighbour A to the right. Both of these atoms have their d_{xz} -orbitals hybridized with the $4p_x$ -orbital of the As atom standing between, so a hopping between these Fe atoms is enabled via intermediate As atom. This hopping gives rise to the indirect superexchange coupling J_2 [15]. By the same mechanism, the indirect exchange between $d_{x^2-y^2}$ -orbitals of neighboring Fe atoms, due to their overlap with p -orbitals of As, yields ferromagnetic nearest-neighbor contribution to J_1 [16,17]. Our earlier analysis suggests that the total J_1 is significantly smaller than J_2 ($\zeta = |J_1|/J_2 \ll 1$). At such a high ratio of frustrating AF couplings, the AF ordering takes place individually on A and B sublattices [18] irrespective of the sign of J_1 . At the mean-field level, the

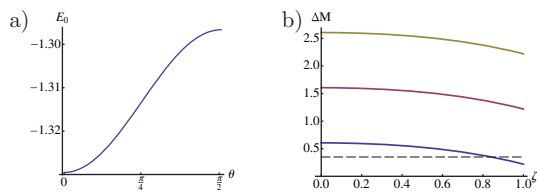


Fig. 4: (Colour on-line) (a) The zero-point energy in units of J_2SN as a function of angle θ between two staggered magnetizations, with $\zeta = 0.5$ [19]. The energy is the lowest for $\theta = 0, \pi$. (b) The staggered magnetization in units of μ_B per unit cell is plotted for three different spin values $S = 1/2, 1$, and $3/2$ (from bottom to top, respectively). The dashed line corresponds to the experimentally observed value of $0.35\mu_B$ [13].

relative order on the two sublattices does not affect the ground-state energy. This implies that, on classical level, the ground state is degenerate, its energy being independent of the angle θ between magnetizations on lattices A and B. Thus, we include excitations —spin-waves— and investigate how they affect the ground state. Introducing standard Holstein-Primakoff bosons a , and b on two respective lattices, the following Hamiltonian is obtained:

$$\begin{aligned} \hat{H} = 2SJ_2 \sum_{\mathbf{k}} & \left\{ 2 \left(a_{\mathbf{k}}^\dagger a_{\mathbf{k}} + b_{\mathbf{k}}^\dagger b_{\mathbf{k}} \right) - (\cos k_x + \cos k_y) \right. \\ & \times \left(a_{\mathbf{k}}^\dagger a_{-\mathbf{k}}^\dagger + b_{\mathbf{k}}^\dagger b_{-\mathbf{k}}^\dagger \right) + 2\zeta \left(\cos \frac{k_x}{2} \cos \frac{k_y}{2} \right) \left(a_{\mathbf{k}}^\dagger b_{\mathbf{k}} - a_{\mathbf{k}}^\dagger b_{-\mathbf{k}}^\dagger \right) \\ & \left. - 2\zeta \cos \theta \left(\sin \frac{k_x}{2} \sin \frac{k_y}{2} \right) \left(a_{\mathbf{k}}^\dagger b_{\mathbf{k}} + a_{\mathbf{k}}^\dagger b_{-\mathbf{k}}^\dagger \right) \right\} + \text{h.c.} \end{aligned} \quad (8)$$

The Bogoliubov transformation of the Hamiltonian (8) yields two new excitations whose dispersions are given by

$$\begin{aligned} E_{\mathbf{k}}^\pm = 4SJ_2 & \left[\left(2 + \cos k_x + \cos k_y \pm 2\zeta \cos \frac{k_x}{2} \cos \frac{k_y}{2} \right) \right. \\ & \left. \times \left(2 - \cos k_x - \cos k_y \pm 2\zeta \cos \theta \sin \frac{k_x}{2} \sin \frac{k_y}{2} \right) \right]^{\frac{1}{2}}. \end{aligned} \quad (9)$$

We numerically determine the zero-point energy (fig. 4(a)). The energy is minimized when the spins on two sublattices are collinear in agreement with the experiments [20].

The staggered magnetization must be evaluated numerically. Figure 4(b) shows the magnetization (per iron site) due to quantum fluctuations as a function of ζ for different values of spin S . The fluctuations are spin independent, but the magnetization is not. Unrealistically low spin and large ζ are required in order to explain what is observed experimentally [13], thus hinting at significant itinerancy in the AF state, in line with our previous arguments.

We now turn to the superconductivity itself, clearly the most difficult problem. It is naturally tempting to use the above propensity for SDW at $\mathbf{q} = \mathbf{M}$ in the parent compound to generate pairing interaction once the system is doped away from the AF order [21]. Following the example of *electron*-doped cuprates and various organic superconductors, this would imply an ordering of a *nodeless* kind, with electron and hole pockets fully gapped but with gap functions of different relative sign [8]. It is important

to stress here the crucial role played by the Josephson-like interband scattering between hole and electron Fermi surfaces in bringing about this form of superconductivity [14]. Since hole and electron pockets are not identical, the gap magnitudes would not be either, but the difference could be quite small. Observing such a relative sign difference in the otherwise fully gapped state (an $s\pm$ or s' state) would clearly be strong boost for this picture of superconductivity generated entirely by antiferromagnetic (SDW) spin fluctuations. However, the above change in sign implies sensitivity to *ordinary* (non-magnetic) impurity disorder which could severely suppress T_c and the gap. This effect, while still present on general grounds, appears less consequential in *hole*-doped cuprates, due to their strongly correlated, almost local nature. In Fe-based superconductors the correlations are not that strong, as we have just argued above, and this impurity sensitivity becomes an important issue. Finally, in order to generate the $s\pm$ (or s') superconducting state, the interband interaction —enhanced by the proximity to the SDW— must overcome the *intra*band repulsion, not an easy task [14].

In light of this, one should not out of hand dismiss the possibility that Fe-based superconductors are of entirely different kind from even the *electron*-doped cuprates and similar superconductors, where the purely *repulsive* interactions suffice to generate pairing near a magnetic instability. Their multiband nature could instead be a realization of the exciton-assisted superconductivity. The phonon interaction appears to be too weak to push T_c to 55 K *by itself* [8]. However, large number of highly polarizable bands around the Fermi surface leads to strong metallic screening and a possibility of a *dynamical* overscreening, which turns μ , the familiar Coulomb pseudopotential of the Eliashberg theory, *attractive* in the certain *finite* wave vector and frequency regions. This would pave the way for the exciton-assisted superconductivity, long-anticipated but never unambiguously observed [22]. The basic idea is that the dynamical Coulomb interaction,

$$V(\mathbf{q}, \omega) = \frac{V(\mathbf{q})}{\epsilon(\mathbf{q}, \omega)}, \quad \epsilon(\mathbf{q}, \omega) = 1 + V(\mathbf{q})\chi_\rho(\mathbf{q}, \omega), \quad (10)$$

($V(\mathbf{q}) = 4\pi e^2/q^2$) turns attractive at some finite \mathbf{q} and relatively low ω . Fe-based superconductors appear to have all the ingredients: their highly polarizable multiband Fermi surface produces *neutral* plasmon modes corresponding to electron and hole densities oscillating in phase (neutral plasmons). Such modes act as “phonons”, particularly if m_e and m_h are sufficiently different. Furthermore, the nesting features lead to enhanced density response $\chi_\rho(\mathbf{q}, \omega)$ near $\mathbf{q} = \mathbf{M}$ and this could turn the effective interaction attractive at relatively low ω . Finally, the interband pairing [23] could still be essential, and acts to further boost T_c *irrespective* of its sign:

$$T_c \sim \omega_p \exp \left\{ -\frac{\frac{1}{2}(\lambda_{ee} + \lambda_{hh})}{\lambda_{ee}\lambda_{hh} - \lambda_{eh}^2} + \frac{[\lambda_{eh}^2 + \frac{1}{4}(\lambda_{ee} - \lambda_{hh})^2]^{\frac{1}{2}}}{\lambda_{ee}\lambda_{hh} - \lambda_{eh}^2} \right\}, \quad (11)$$

where $\lambda_{ee(hh)}$ and λ_{eh} are the e-e (h-h) and the interband coupling constants, respectively, and ω_p is the characteristic frequency of the exciton-assisted pairing. T_c generated by this mechanism is notoriously difficult to estimate, both due to the competition from structural and covalent instabilities in the p-h channel and the need to consider local-field contributions to $\epsilon(\mathbf{q}, \omega)$ [24]. Nevertheless, this “hybrid” option—in which phonons help make *intra*band interactions attractive, or at least only weakly repulsive, and enable the magnetically enhanced repulsive *inter*band interactions provide the crucial boost to T_c —should be kept in mind as the experimental and theoretical investigations of Fe-based superconductivity continue in earnest.

In summary, Fe-based superconductors appear to offer a glimpse of a new road toward room-temperature superconductivity. We have constructed a tight-binding model which qualitatively describes the physics of FeAs layers where the superconductivity apparently resides. Analytical results were given for the elementary particle-hole response in charge, spin and multiband channels and used to discuss various features of the SDW/AF order and superconductivity. We stress the importance of puckering of As atoms in promoting *d* electron itinerancy and argue that the high T_c of Fe-based superconductors might be essentially tied to the multiband character of their Fermi surface, favorable to the $s\pm$ (or s') superconducting state. It is tempting to speculate that different T_c 's obtained for different rare-earth substitutions might be related to the different amount of puckering in FeAs layers and regulating this amount might be the key to even higher T_c .

The authors are grateful to I. MAZIN, C. BROHOLM and C. L. CHIEN for useful discussions. This work was supported in part by the NSF grant DMR-0531159. Work at the Johns Hopkins Institute for Quantum Matter is supported by the U. S. Department of Energy Office of Science under Contract No. DE-FG02-08ER46544.

Additional remark: Since this manuscript was posted on the arXiv in April 2008 (arXiv:0804.4678) there were numerous significant experimental and theoretical developments in this exceptionally fast-paced field. Those most relevant to this work include the observation of the superconducting gap in PCAR [25] and ARPES experiments [26–28] and various theoretical approaches exemplified by refs. [29–35]. Especially notable among these are further theoretical explorations of the $s\pm$ (or s') superconducting state in refs. [14,36–38].

REFERENCES

- [1] KAMIHARA Y. *et al.*, *J. Am. Chem. Soc.*, **128** (2006) 10012.
- [2] KAMIHARA Y. *et al.*, *J. Am. Chem. Soc.*, **130** (2008) 3296.
- [3] CHEN X. H. *et al.*, *Nature*, **453** (2008) 761; CHEN G. F. *et al.*, *Phys. Rev. Lett.*, **100** (2008) 247002; REN Z.-A. *et al.*, *EPL*, **82** (2008) 57002; REN Z.-A. *et al.*, *Mater. Res. Innov.*, **12** (2008) 105.
- [4] QUEBE P., TERBÜCHTE L. J. and JEITSCHKO W., *J. Alloys Compd.*, **302** (2000) 70.
- [5] LI T., arXiv:0804.0536 preprint (2008).
- [6] LEBÈGUE S., *Phys. Rev. B*, **75** (2007) 035110.
- [7] HAULE K., SHIM J. H. and KOTLIAR G., *Phys. Rev. Lett.*, **100** (2008) 226402; HAULE K. and KOTLIAR G., arXiv:0805.0722 preprint (2008).
- [8] MAZIN I. I., SINGH D. J., JOHANNES M. D. and DU M. H., *Phys. Rev. Lett.*, **101** (2008) 057003.
- [9] KUROKI K. *et al.*, *Phys. Rev. Lett.*, **101** (2008) 087004.
- [10] CAO C., HIRSCHFELD P. J. and CHENG H.-P., *Phys. Rev. B*, **77** (2008) 220506(R).
- [11] RAGHU S. *et al.*, *Phys. Rev. B*, **77** (2008) 220503(R); QI X.-L. *et al.*, arXiv:0804.4332 preprint (2008).
- [12] KORSHUNOV M. M. and EREMIN I., *EPL*, **83** (2008) 67003.
- [13] DE LA CRUZ C. *et al.*, *Nature*, **453** (2008) 899.
- [14] CVETKOVIC V. and TESANOVIC Z., arXiv:0808.3742 preprint (2008).
- [15] YILDIRIM T., *Phys. Rev. Lett.*, **101** (2008) 057010.
- [16] SI Q. and ABRAHAMS E., *Phys. Rev. Lett.*, **101** (2008) 076401.
- [17] MANOUSAKIS E. *et al.*, *Phys. Rev. B*, **78** (2008) 205112.
- [18] CHANDRA P. and DOUCOT B., *Phys. Rev. B*, **38** (1988) 9335.
- [19] MA F., LU Z.-Y. and XIANG T., *Phys. Rev. B*, **78** (2008) 224517.
- [20] CHANDRA P., COLEMAN P. and LARKIN I., *Phys. Rev. Lett.*, **64** (1990) 88.
- [21] SCALAPINO D. J., LOH E. jr. and HIRSCH J. E., *Phys. Rev. B*, **34** (1986) 8190.
- [22] GINZBURG V. L. and KIRZHNITS D. A., *High-Temperature Superconductivity* (Consultants Bureau, New York) 1982.
- [23] SUHL H., MATTHIAS B. T. and WALKER L. R., *Phys. Rev. Lett.*, **3** (1959) 552.
- [24] LITTLEWOOD P. B., *Phys. Rev. B*, **42** (1990) 10075.
- [25] CHEN T. Y. *et al.*, *Nature*, **453** (2008) 1224.
- [26] DING H. *et al.*, *EPL*, **83** (2008) 47001.
- [27] WRAY L. *et al.*, *Phys. Rev. B*, **78** (2008) 184508; arXiv:0808.2185 preprint (2008).
- [28] KONDO T. *et al.*, *Phys. Rev. Lett.*, **101** (2008) 147003.
- [29] GIOVANNETTI G., KUMAR S. and VAN DEN BRINK J., *Phys. B*, **403** (2008) 3653.
- [30] RAN Y. *et al.*, arXiv:0805.3535 preprint (2008); WANG F. *et al.*, arXiv:0805.3343 preprint (2008); WANG F. *et al.*, *Phys. Rev. Lett.*, **102** (2009) 047005.
- [31] SKNEPNEK R. *et al.*, arXiv:0807.4566, to be published in *Phys. Rev. B*.
- [32] LINDER J. and SUDBØ A., arXiv:0811.1775 preprint (2008).
- [33] KULIC M., DRECHSLER S.-L. and DOLGOV O. V., arXiv:0811.3119 preprint (2008).
- [34] BELASHCHENKO K. D. and ANTROPOV V. P., *Phys. Rev. B*, **78** (2008) 212515.
- [35] PODOLSKY D., KEE H. Y. and YONG B. K., arXiv:0812.2907 preprint (2008).
- [36] CHUBUKOV A. V., EFREMOV D. and EREMIN I., *Phys. Rev. B*, **78** (2008) 134512.
- [37] PARISH M. M., HU J. and BERNEVIG B. A., *Phys. Rev. B*, **78** (2008) 144514.
- [38] STANEV V., KANG J. and TESANOVIC Z., *Phys. Rev. B*, **78** (2008) 184509.